ZEUS results on inclusive diffraction

Heuijin Lim (on behalf of the ZEUS Collaboration)

DESY Notkestr 85. D-22607 Hamburg, Germany

Abstract. Deep inelastic diffractive scattering, $ep \rightarrow e'\gamma^* p \rightarrow e'XN$, has been studied at HERA with the ZEUS detector in a wide kinematic range in the $\gamma^* p$ centre-of-mass energy W, the photon virtuality Q^2 and the mass of the system X, M_X. ZEUS results on diffraction have been obtained using the M_X method and by identifying leading protons which carry a large fraction of the incoming proton beam energy. They are presented in terms of the diffractive cross section, $d\sigma(M_X, W, Q^2)/dM_X$ and the diffractive structure function, $x_{IP}F_2^{D(3)}(\beta, x_{IP}, Q^2)$.

Keywords: diffractive deep inelastic scattering, QCD
PACS: 13.60.Hb, 12.38.-t

INTRODUCTION

In the Quantum Chromodynamics (QCD) picture, diffraction, where the proton or a low-mass nucleonic system emerges from the interaction with almost the full energy of the incident proton, is mediated by the exchange of a colour singlet carrying the quantum numbers of the vacuum, called the Pomeron, which in lowest order could be a two-quark or two-gluon system.

ZEUS diffractive results measured in two different analyses have recently been published. One uses data taken in 1998-1999 with the forward plug calorimeter (FPC) installed in the $20 \times 20\,\text{cm}^2$ beam hole of the forward uranium calorimeter [1]. The FPC increased the calorimetric coverage in the outgoing proton beam direction by about one unit in pseudorapidity and expanded the accessible range in M_X by a factor of about 1.7. It also substantially limited the contribution from the nucleon dissociation to $M_N < 2.3$ GeV. Diffractive events were selected using the M_X method which is based on the different characteristics of the M_X distributions in diffractive and non-diffractive processes. Results are presented for $\gamma^* p \rightarrow XN$, $M_N < 2.3$ GeV in the range $2.2 < Q^2 < 80$ GeV^2, $37 < W < 245$ GeV and $M_X < 35$ GeV. The other analysis uses the leading proton spectrometer (LPS) to detect the scattered protons, carrying at least 90 % of the incoming proton momentum. Based on data taken in 1997, results are presented for $\gamma^* p \rightarrow Xp$ in the range $0.03 < Q^2 < 100$ GeV^2, $25 < W < 240$ GeV and $M_X > 1.5$ GeV [2].

DIFFRACTIVE CROSS SECTION

The LPS analysis shows that the diffractive cross section falls steeply with the squared four-momentum transfer at the proton vertex, t. Fitting the distribution with a function of the form, $d\sigma_{\gamma^* p \rightarrow Xp}/dt \propto e^{b|t|}$, yields $b = 7.9 \pm 0.5(\text{stat.})^{+0.8}_{-0.5}(\text{syst.})$ GeV^{-2}. This value is compatible with b-value measured for elastic pion-proton scattering [3].

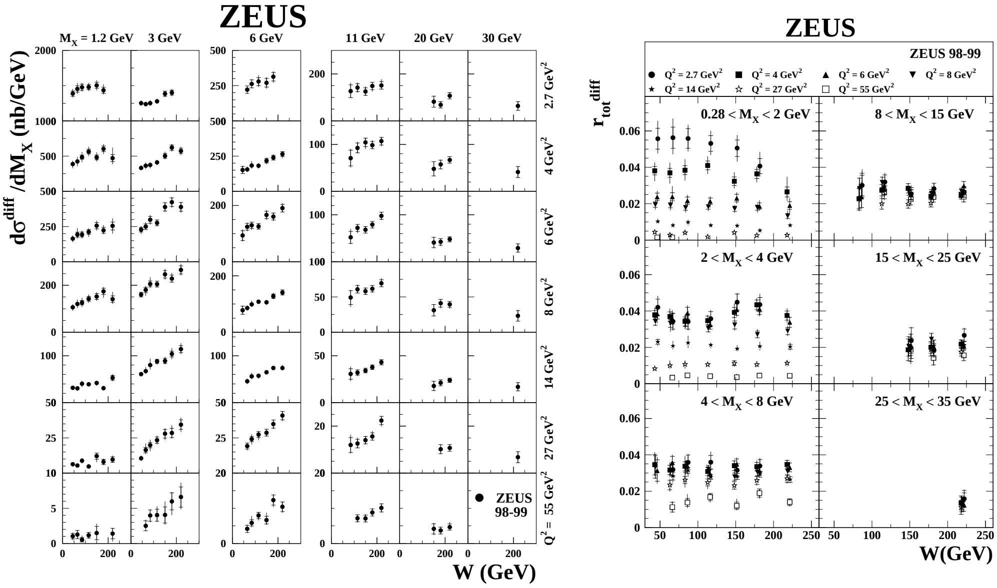

FIGURE 1. (left) Diffractive cross section from FPC. (right) Ratio $r_{\rm tot}^{\rm diff} = \sigma^{\rm diff}/\sigma_{\gamma^* p}^{\rm tot}$ from FPC.

Figure 1-(left) shows the diffractive cross section $d\sigma^{\rm diff}_{\gamma^* p\to XN, M_N<2.3{\rm GeV}}/dM_X$ measured in the FPC analysis as a function of W for different Q^2 and M_X. For $M_X < 2$ GeV, the diffractive cross section is rather constant with W while at higher M_X, a strong rise with W is observed for all values of Q^2. This rise was quantified by fitting the data in the range $2 < M_X < 15$ GeV and in different Q^2 intervals with the form, $d\sigma^{\rm diff}/dM_X = c(M_X,Q^2)\cdot(W/W_0)^{4(\overline{\alpha_{I\!P}}(Q^2)-1)}$ where $c(M_X,Q^2)$ and $\overline{\alpha_{I\!P}}(Q^2)$ were treated as free parameters. Assuming $d\sigma/dt \propto e^{b|t|}$ and $\alpha_{I\!P}(t) = \alpha_{I\!P}(0) + \alpha'_{I\!P}\cdot t$, it leads to $\alpha_{I\!P}(0) = \overline{\alpha_{I\!P}} + \alpha'_{I\!P}/b$. The Pomeron intercept rises by $\Delta\alpha^{\rm diff}_{I\!P} = 0.0741 \pm 0.0140({\rm stat.})^{+0.0047}_{-0.0100}({\rm syst.})$ between Q^2 of 7.8 and 27 GeV^2. This establishes a Q^2 dependence of the Pomeron intercept and shows that diffractive DIS like inclusive DIS processes, cannot be interpreted as resulting from single Pomeron exchange combined with the assumption of Regge factorisation.

The ratio $r^{\rm diff}_{\rm tot} \equiv (\int_{M_a}^{M_b} dM_X d\sigma^{\rm diff}_{\gamma^* p\to XN, M_N<2.3{\rm GeV}}/dM_X)/\sigma^{\rm tot}_{\gamma^* p}$ was determined in all M_X bins and is shown in fig. 1-(right). For $M_X < 2$ GeV, $r^{\rm diff}_{\rm tot}$ falls with W, while at the higher M_X, it is approximately constant. It agrees with the conclusion that for $M_X < 2$ GeV, $\alpha^{\rm diff}_{I\!P}(0)$ is compatible with the soft Pomeron and for larger M_X, $\alpha^{\rm diff}_{I\!P}(0)$ increases with Q^2, invalidating the idea of single Pomeron exchange. The low M_X bins exhibit a strong decrease of $r^{\rm diff}_{\rm tot}$ with increasing Q^2, while for $M_X > 4$ GeV, this decrease becomes less dramatic and for $M_X > 8$ almost disappears. The diffractive cross section for $0.28 < M_X < 2$ GeV shows a much stronger decrease than $1/Q^2$, which is characteristic of a higher twist behavior. For $M_X > 8$ GeV, the cross section decreases as $1/Q^2$, consistent with a leading twist behavior. For the highest W bin ($200 < W < 245$ GeV), the ratio $\sigma^{\rm diff}$ ($0.28 < M_X < 35$ GeV, $M_N < 2.3$ GeV)$/\sigma^{\rm tot}$ reaches $15.8^{+1.2}_{-1.0}$ % at $Q^2 = 4$ GeV^2 and decreases slowly with Q^2, reaching $9.6^{+0.7}_{-0.7}$ % at $Q^2 = 27$ GeV^2.

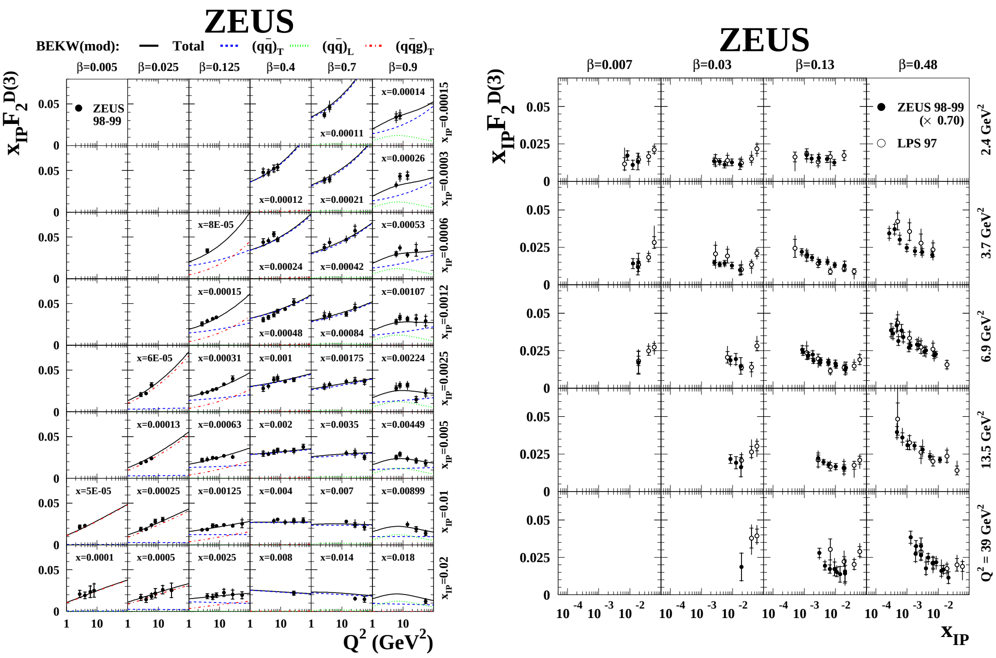

FIGURE 2. (left) $x_{IP}F_2^{D(3)}$ from the FPC analysis. The lines are the results of BEKW(mod) fit. (right) $x_{IP}F_2^{D(3)}$ from the FPC analysis compared with the results of LPS measurement.

Diffractive processes account for a substantial part of the total deep inelastic cross section.

DIFFRACTIVE STRUCTURE FUNCTION

The diffractive analogue to the proton structure function F_2, the diffractive structure function $F_2^{D(3)}$ is parametrized in terms of Q^2, the momentum fraction $x_{IP} = (M_X^2 + Q^2)/(W^2 + Q^2)$ of the proton carried by the Pomeron, and the momentum fraction $\beta = Q^2/(M_X^2 + Q^2)$ of the Pomeron carried by the struck quark. If $F_2^{D(3)}$ is interpreted in terms of quark densities, it specifies the probability to find, in a proton undergoing a diffractive reaction, a quark carrying a fraction $x = \beta x_{IP}$ of the proton momentum.

Figure 2-(left) shows $x_{IP}F_2^{D(3)}$ as a function of Q^2 for different values of β and x_{IP}. For $\beta = 0.9$, the region dominated by diffractive production of states with $M_X < 2$ GeV, $x_{IP}F_2^{D(3)}$ is constant or slowly decreasing with Q^2 due to higher twist effects in longitudinal diffractive $\gamma^* p$ scattering. For $\beta \leq 0.7$ and $x = \beta x_{IP} < 0.002$, positive scaling violations are observed presumably due to perturbative effects such as gluon emission. For fixed β, the Q^2 dependence of $x_{IP}F_2^{D(3)}$ changes with x_{IP}. This is inconsistent with the hypothesis that single Pomeron exchange is responsible for these data.

Comparison with the LPS data shows that about 30 % of the FPC cross section comes from nucleon dissociation with $M_N < 2.3$ GeV. Figure 2-(right) compares the LPS data with the FPC data multiplied by a factor of 0.7. Good agreement between two

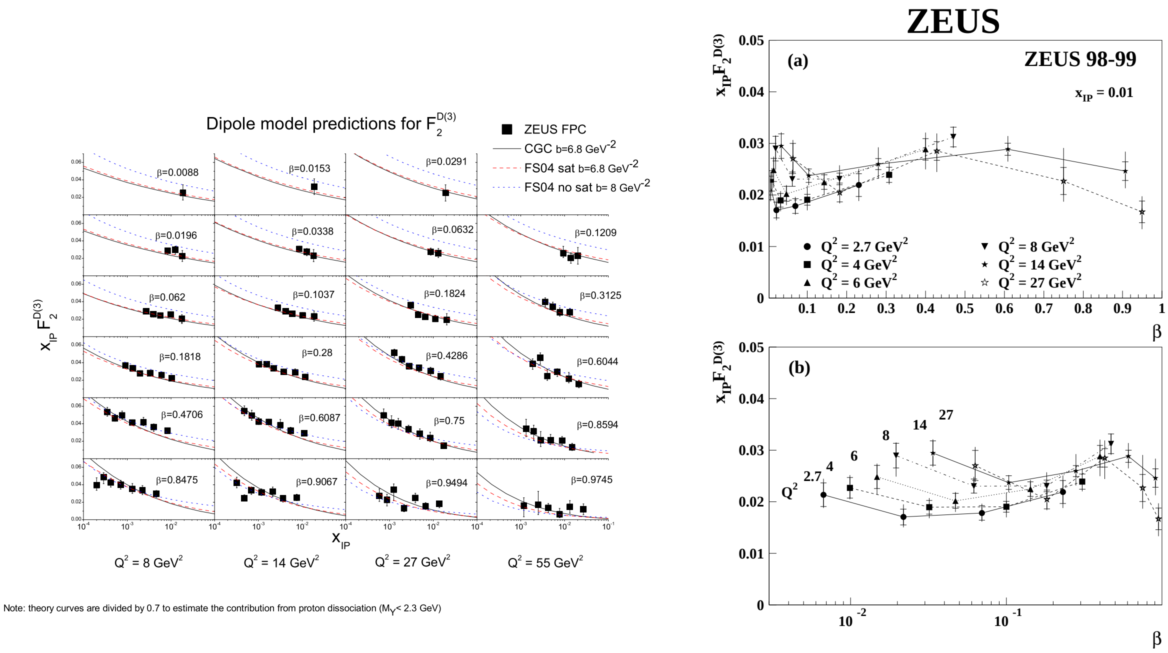

FIGURE 3. (left) $x_{IP}F_2^{D(3)}$ compared with FS04 model without saturation (dotted line), FS04 model with saturation (dashed line) and CGC model (solid line). (right) $x_{IP}F_2^{D(3)}$ for $x_{IP} = 0.01$ from FPC.

measurements is observed, with the possible exception of the region of $x_{IP} > 0.01$, where LPS data include contributions from Reggeon exchange.

The data were compared with a colour dipole model assuming that the virtual photon fluctuates into a colour dipole ($q\bar{q}$ or $q\bar{q}g$) which interacts with the proton by the exchange of a colourless object. The BEKW(mod) fit describes the data well (fig. 2-(left)). As shown in fig. 3-(left), the Forshaw and Shaw (FS04) model without saturation overestimates the diffractive contribution somewhat for the low β region where the contribution of gluon is dominant. The FS04 model with saturation and and the Colour Glass Condensate (CGC) model give good descriptions of the data [4].

Figure 3-(right) shows $x_{IP}F_2^{D(3)}$ for fixed $x_{IP} \equiv x_0 = 0.01$ as a function of β for different values of Q^2. The $x_{IP}F_2^{D(3)}$ have a maximum near $\beta = 0.5$, consistent with a $\beta(1-\beta)$ variation which is explained in the dipole models of diffraction by $\gamma^* \rightarrow q\bar{q}$ splitting and two-gluon exchange. The rise of $x_{IP}F_2^{D(3)}$ as $\beta \rightarrow 0$ and its increase with Q^2 is reminiscent of the logarithmic scaling violations observed in F_2 at low x, which arises from QCD evolution.

REFERENCES

1. ZEUS Collaboration; S. Chekanov *et al.*, Nucl. Phys. **B 713**, 3 (2005).
2. ZEUS Collaboration; S. Chekanov *et al.*, Eur. Phys. J. **C 38**, 43 (2004).
3. K. Goulianos, Phys. Rep. **101**, 169 (1983).
4. J. R. Forshaw and G. Shaw, JHEP 0412 (2004) 052 and hep-ph/0411337.